JMEPEG (2007) 16:86–92
DOI: 10.1007/s11665-006-9013-z

1059-9495/$19.00

Residual Stress Evaluation of AA2024-T3 Friction Stir Welded Joints

M.T. Milan, W.W. Bose Filho, J.R. Tarpani, A.M.S. Malafaia, C.P.O. Silva, B.C. Pellizer and L.E. Pereira

(Submitted January 6, 2005; in revised form January 16, 2006)

The main aim of this study was to evaluate the residual stress field in friction stir welded joints of 2024-T3 aluminum alloy plates using the slitting method. This is based on the fact that when a cut, simulating a growing crack, is incrementally introduced into a part, residual stresses are relieved on the slot surfaces created, causing the part to deform. Such deformation can be measured by strain gages attached to specific regions of the part and the residual stress profile that originally existed can be evaluated. Cuts were introduced by wire electro discharge machining (WEDM), in finishing mode, either perpendicularly or longitudinally to the weld nugget, in $3.2 \times 60 \times 120$ mm^3 rectangular testpieces. For the longitudinal testpieces, the slot was introduced in two different positions: on the center of the weld nugget and 5 mm distant from the weld center line, in order to sample the thermomechanically/heat affected zone. The residual stress intensity factor, K_r, was calculated using a fracture mechanics approach and the inverse weight function method was employed to obtain the initial residual stress profile. Residual stress redistribution profiles ahead of the slot tip could also be derived using the inverse weight function method. However, for cracked components subjected to compressive residual stress fields, when the crack faces are in contact, a non-linear problem arises and the zero displacement condition has to be taken into account in order to provide a more accurate solution of the residual stress field.

Keywords aluminum alloys, friction stir welding, residual stresses, slitting method

1. Introduction

In recent years, friction stir welding has been considered as potential candidate to replace conventional riveting operations in aircraft manufacture. However, it is well-known that residual stresses are present in welded structures after fabrication. These residual stresses are likely to affect mechanical and corrosion properties of the materials and therefore to influence the in-service performance of structural components. The effects of residual stresses on the fatigue crack propagation have been reported by several authors (Ref 1-7). Tensile residual stresses increase the crack growth rate by an increase in the effective stress ratio. On the other hand, compressive residual stresses reduce the fatigue crack growth rate by decreasing the stress intensity factor range and/or stress ratio. Additionally, residual stresses were found to affect initiation fracture toughness values of aluminum alloys (Ref 8, 9).

M.T. Milan, W.W. Bose Filho, J.R. Tarpani, A.M.S. Malafaia, C.P.O. Silva and **B.C. Pellizer**, Department of Materials, Aeronautics and Automotive Engineering, Engineering School of São Carlos, NEMAF – Núcleo de Ensaios de Materiais e Análises de Falhas, University of São Paulo, CEP: 13566-590 São Carlos, SP, Brazil; and **L.E. Pereira**, Department of Materials Engineering, EMBRAER S/A, CEP: 12227-901 São José dos Campos, SP, Brazil. Contact e-mail: mtmilan@sc.usp.br.

The main aim of this paper was to measure the residual stresses in AA2024-T3 friction stir welded joints provided by EMBRAER (Brazil), both longitudinally and perpendicularly to the welding line, using the slitting method. Additionally, residual stress redistribution profiles ahead of the slot were determined for several slot lengths, simulating the growth of the slot into the residual stress field. The results obtained represent valuable information for understanding fatigue and fracture

List of symbols

a	crack or slot length
$A_{v,\mu}$	weight function coefficients
d	slot width
e	elongation
E	Young's modulus
$h(x,a)$	weight function
K_r	residual stress intensity factor
K_{rx}	longitudinal residual stress intensity factor
K_{ry}	transverse residual stress intensity factor
L	length of the testpiece
M	position of the strain gage
RA	reduction in area
UTS	ultimate tensile strength
W	width of the testpiece
$Z(a)$	influence function
ε	strain
$d\varepsilon/da$	strain derivative
$\mu\ \varepsilon$	microstrain
σ_r	residual stress
σ_y	0.2% offset yield strength
σ_{rx}	longitudinal residual stress
σ_{ry}	transverse residual stress

toughness properties of friction stir welded alloys if a damage tolerant design is employed.

2. The Slitting Method

The slitting method is a powerful and easy to implement technique employed to determine both near surface and through the thickness residual stress profiles. It is based on the fact that when a cut, simulating a growing crack, is incrementally introduced into a part, the residual stresses are relieved on the slot surfaces created, causing the part to deform. Such deformation can be measured by strain gages attached to specific regions of the part (Fig. 1) and the residual stress profile that originally existed can be evaluated (Ref 10).

Assuming a narrow slot ($d << a$), linear elastic fracture mechanics equations can be employed to establish a relationship between the measured strains, ε, and the corresponding residual stress intensity factor, K_r (Ref 11):

$$K_{Ir}(a) = \frac{E'}{Z(a)} \frac{d\varepsilon_M}{da} \quad \text{(Eq 1)}$$

where ε_M is the measured strain at point M during the cutting procedure, a is the slot length, E' is the generalized form of the Young's modulus ($E' = E$ for plane stress and $E' = E/(1-\nu^2)$ for plane strain) and $Z(a)$ is the "influence function" which depends on the testpiece geometry, cut plane location and strain measurement position, but it is independent on the residual stress profile.

For a rectangular plate, where $L > 2W$, and taking strain measurements at the back face point M, $Z(a)$ is given as (Ref 12):

for $a/W < 0.2$

$$Z(a) = r\frac{-2,532}{(W-a)^{1.5}}\sqrt{1-25\cdot\left(\frac{a}{W}-0.2\right)^2} \cdot\left[5.926\cdot\left(0.2-\frac{a}{W}\right)^2 - 0.288\cdot\left(0.2-\frac{a}{W}\right)+1\right] \quad \text{(Eq 2)}$$

for $0.2 < a/W < 1$

$$Z(a) = \frac{-2.532}{(W-a)^{1.5}} \quad \text{(Eq 3)}$$

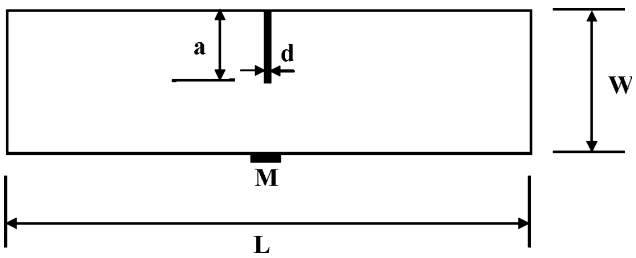

Fig. 1 Rectangular plate containing a cut along its center plane, strain measurement taken at the point M

$K_{Ir}(a)$ and the normal residual stresses, $\sigma_r(x)$, that existed prior to the cutting (where the x axis is coincident with the cut plane) can be correlated by the following expression:

$$K_{Ir}(a) = \int_{a_o}^{a} h(x,a)\cdot\sigma_r(x)\cdot dx \quad \text{(Eq 4)}$$

where $h(x,a)$ is the weight function, which is available for several geometries (Ref 13). In particular, for a single edge crack in a finite width rectangular plate, the weight function is given as

$$h(x,a) = \sqrt{\frac{2}{\pi a}}\frac{1}{\sqrt{1-x/a}} \left[1+\frac{1}{(1-a/W)^{3/2}}\sum_{v,\mu} A_{v,\mu}(a/W)^{\mu}(1-x/a)^{v+1}\right] \quad \text{(Eq 5)}$$

where $A_{v,\mu}$ values are found in Table 1 (Ref 13).

Knowledge of $K_{Ir}(a)$ profile (obtained by Eq 1) makes possible to calculate $\sigma_r(x)$ profile through the inversion of Eq 4. One of the methods used for such purpose is the incremental stress method (Ref 11), where the stress profile is approximated by a series of small steps as depicted schematically in Fig. 2. The stress level in each step can be calculated by applying Eq 4 to a hypothetical, incrementally prolonging crack. This leads to a discrete form of Eq 4:

$$K_r(a_i) = \sum_{j=1}^{i}\sigma_j\int_{a_{j-1}}^{a_j} h(x,a_i)dx \quad \text{(Eq 6)}$$

Using Eq 6 sequentially allows each σ_j to be determined and the stress profile can be determined. The resulting stress distribution converges to the exact solution $\sigma_r(x)$ as $\triangle a \to 0$. The procedure described above is able not only to determine the initial residual stress profile that was present in the material before the slot was introduced, but also the redistributing stress profiles ahead of the slot tip, by simply changing the integration limits in Eq 6, i.e., using different values of initial slot lengths, provided that linear elastic conditions remain valid.

3. Experimental Procedure

Plates of AA2024-T3, 3.2 mm thick were friction stir welded along the rolling direction. Mechanical properties of the material are provided in Table 2. Welding parameters are proprietary to EMBRAER. Then, 60×120 mm^2 rectangular testpieces were machined by wire electro discharge machining (WEDM) in two different configurations, as represented in Fig. 3.

Table 1 Weight function coefficients for rectangular testpieces (Ref 4)

ν	μ = 0	μ = 1	μ = 2	μ = 3	μ = 4
0	0.4980	2.4463	0.0700	1.3187	−3.067
1	0.5416	−5.0806	24.3447	−32.7208	18.1214
2	−0.19277	2.55863	−12.6415	19.7630	−10.986

A strain gage, with gage length of 2 mm, was bonded to the back face of each testpiece, in a configuration similar to the one presented in Fig. 3. A plastic resin was applied on top of the strain gage and wires to avoid contact with the environment. Shielded wires were used to connect the strain gages to the strain data acquisition apparatus in order to minimize electromagnetic interferences.

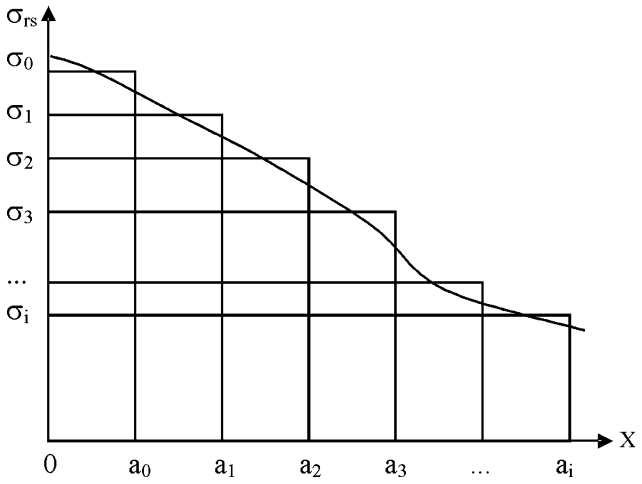

Fig. 2 Stress profile approximation using small constant stress steps

Table 2 Mechanical properties of AA2024-T3 alloy

Material	UTS, MPa	σ_y, MPa	*e*, %	RA, %	*E*, GPa
2024-T3 Transverse	459.3	302.9	21.5	24.5	83.3
	465.4	311.7	21.1	23.0	81.3
	466.0	307.8	21.7	21.6	78.7
Average	463.6	307.5	21.4	23.0	81.1
2024-T3 Longitudinal	473.6	355.7	21.2	18.7	83.8
	481.6	351.2	21.4	20.2	77.9
	475.5	344.0	20.7	23.5	75.2
Average	476.9	350.3	21.1	20.8	79.0

Cutting was performed using a Charmilles 100 WEDM machine, either longitudinally or perpendicularly to the weld line. Width of cut was approximately 0.3 mm. As depicted in Fig. 3b, for longitudinal testpieces, the slot was introduced in two different positions: 0 mm and 5 mm distant from the nugget center line (on the advancing side of the weld), to simulate a crack growing in the weld and in the heat affected zone, respectively. For perpendicular testpieces the slot approached the nugget from the advancing side of the rotating FSW tool. Recent work has found that WEDM is the best choice for introducing the slot, because it is more practical and precise and it is less likely to introduce additional stresses (Ref 14-18). For all tests, increments of 0.5 mm were chosen for each step and the readings were taken 5 min after the slotting procedure in each step had finished.

After the strain data were obtained as a function of the slot length, the secant method was used to calculate $d\varepsilon/da$ values which were employed in Eq 1. After K_r values were found, the residual stress profile was determined by the incremental stress method, using a routine created in Mathcad software. Residual stress redistribution profiles were determined using the same procedure as described above, but changing the initial slot length in the calculations.

4. Results and Discussion

4.1 Transverse Slot Testpieces

Figure 4 shows longitudinal residual stress intensity factor profile, K_{rx} calculated according to Eq 1 for testpieces where the slot was introduced perpendicularly to the weld line. It is observed that there is a "negative" peak value at approximately 14 mm from the edge of the testpiece and K_{rx} remains negative up to the weld center line. In fact, a "negative" K_r does not exist for a closed crack, but it means that when an external load

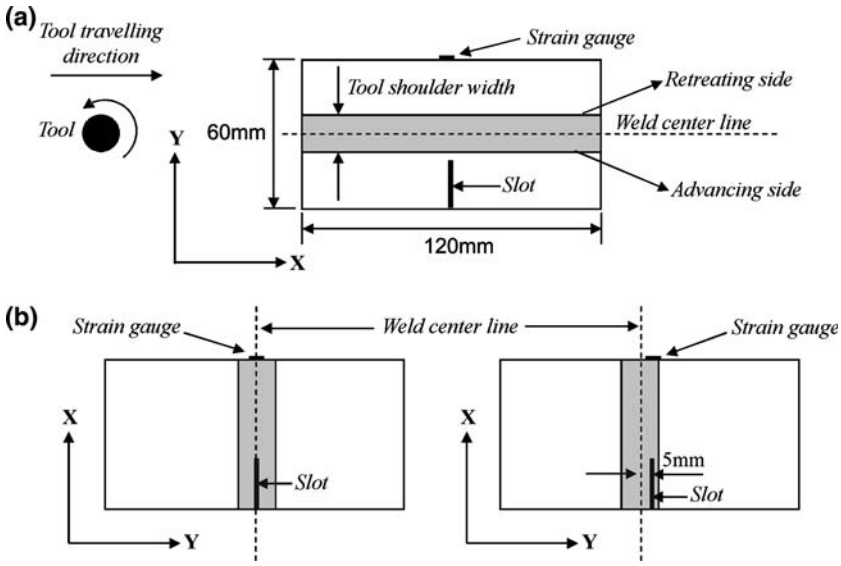

Fig. 3 Testpiece configurations: (a) Transverse testpiece for measuring longitudinal stresses; (b) longitudinal testpiece for measuring transverse stresses, slot at 0 mm (left) and 5 mm from the weld center line. Testpieces presented in (b) present the same dimensions as in (a)

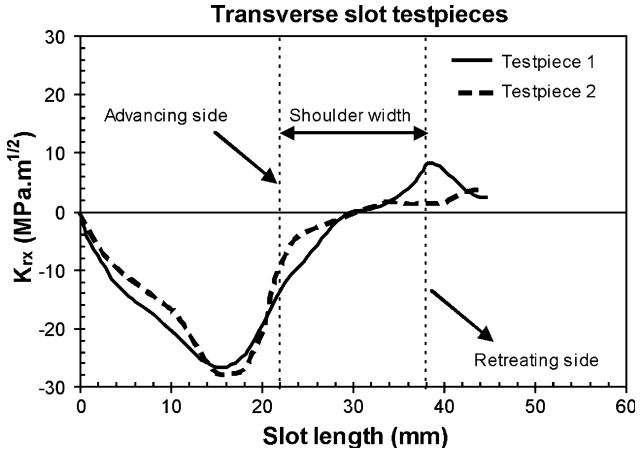

Fig. 4 Residual stress intensity factor profiles for transverse slot testpieces

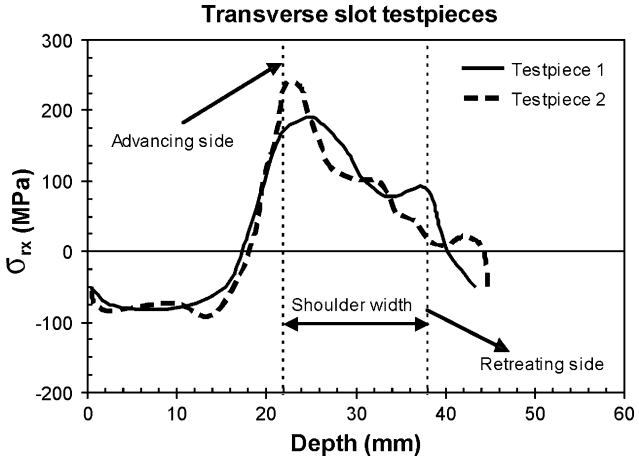

Fig. 5 Residual stress profiles for transverse slot testpieces

is applied, the thermal residual stress profile shields the crack, i.e., effectively reduces the local K. The negative values of K_{rx} are likely to produce strong fatigue crack growth deceleration if a crack approaches perpendicularly to the weld line; however after crossing the weld region, K_{rx} are positive and the crack may accelerate, when compared to parent material behavior. It is important to emphasize that such analysis does not take into account the differences in plastic properties of the different regions of the weld, which may cause crack retardation or acceleration depending if the crack grows into a soft–hard or hard–soft transition, respectively (Ref 6-9). Therefore, when cracks grow in welded structures the effective crack tip driving force will be governed by a competitive interaction of the material intrinsic behavior, residual stresses and plastic mismatch between weld regions.

As aforementioned, Eq 1 is only valid if linear elastic conditions are attained. However, in practical situations, local plasticity ahead of the cut tip and the finite width of the cut may produce non-linear effects. In other words, the strain measured during the cutting process could be not only the response to the released stresses on the slot faces but also caused by localized plastic yielding immediately ahead of the slot tip. Therefore, as proposed by Schindler (Ref 19), a correction procedure based on the effective crack length (a_{eff}) was applied to the data presented in Fig. 4. Details of such procedure are found in Ref 19 and will not be described here, for the sake of simplicity. Results show that the difference between corrected and as-calculated K_r values was found to be insignificant and the correction procedure will not be adopted in this paper.

Using the inverse weight function method, as given by Eq 6, it was possible to obtain the initial residual stress profile that was present in the material before the slot was introduced, as depicted in Fig. 5. Although the trends between the results presented in this work and the literature (Ref 20-23) are the same, a direct comparison seems to be inadequate because the residual stress profile is particularly dependent on testpiece geometry and welding parameters, such as tool geometry and traveling and rotational speeds. Far from the welded region, near the edges of the testpiece, residual stresses are compressive (~−100 MPa). In the welded region there is a peak of tensile residual stress, ranging from 180 MPa to 220 MPa (50–60% of parent material yield strength). The peak is localized in the region corresponding to the transition between thermomechanically and heat affected zones on the advancing side of the weld, at approximately 8 mm from the weld center line. Consequently, this is the most likely region for a fatigue crack to initiate. Although the residual stresses remain tensile on the retreating side of the weld, at an equivalent distance from the weld center line (8 mm), measured values are significantly lower, ranging from 30 MPa to 100 MPa (10–30% of parent material yield strength). Previous works have also shown that the tensile residual stresses on the advancing side of the weld are invariably higher than on the retreating side; however, the authors did not offer any explanation for such phenomenon (Ref 20, 21). Recent work (Ref 21) has shown that, for the same traveling speed, higher rotational speeds produce higher tensile residual stress peaks regions due to the increased frictional heat generation. In this sense, it is possible that the difference in tensile residual stress values in both sides of the weld results from different local heat input rates, depending on the relative motion between the material and the tool. On the advancing side of the weld, as a result of a combination of the rotational and traveling movements, the localized frictional heat generation is likely to be larger because the relative speed of the tool in contact with the material is higher. On the other hand, on the retreating side of the weld, the relative speed of the tool surface is given by the difference in the tangential and traveling speed values, resulting in a lower localized heat generation. However, further work is necessary to confirm the assumptions stated above, including a thermal analysis to determine temperature distribution across the weld region during the welding procedure.

Figure 6 depicts several redistributing residual stress profiles for testpiece 1, simulating the growth of the slot into the residual stress field. As the slot gets longer, the residual stress profile is rearranged in order to maintain equilibrium conditions. Additionally, it is possible to observe that the residual stress value in the vicinity of the slot tip remains negative up to approximately the center of the nugget, although, in the intact testpiece, a positive tensile residual stress field existed in this region. Considering the same distance from the slot tip, it was found that the maximum compressive residual stress is obtained for a slot length of approximately 15 mm, which is in agreement with the "negative" peak K_{rx} value observed at this position. It is important to observe that for slot lengths from

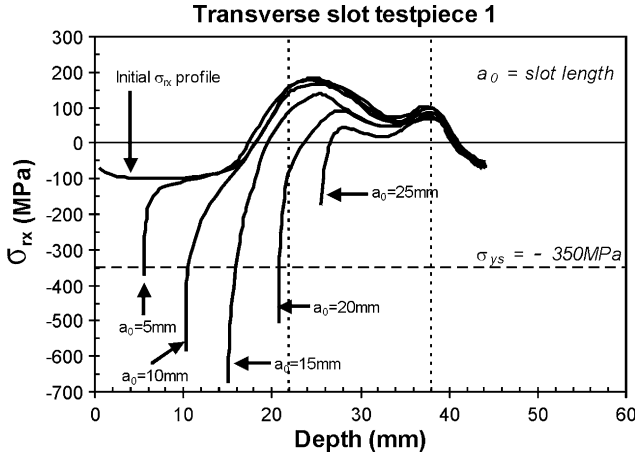

Fig. 6 Residual stress redistribution ahead of the slot tip for transverse slot testpiece 1. Vertical dashed lines represent the shoulder width and the horizontal dashed line indicates the "cut-off" stress given by the compressive yield strength of the material

5 mm to 20 mm, the maximum calculated compressive stress at 0.5 mm from the slot front is larger than the compressive yield strength of the material (~350 MPa, assuming that the yield strength in compression is equal to the value obtained in tension). These singularities are a direct consequence of the inverse weight function analysis, which assumes a linear elastic perfect material. In principle, the true stress profile in the vicinity of the slot shall be bounded by the compressive yield strength of the material, establishing a "cut-off" stress. Therefore, the true stress profiles will be slightly different from those presented in Fig. 5, because the area excluded below the "cut-off" stress has to be redistributed within the rest of the curve. However, since this area is normally very narrow, the differences are likely to be insignificant and the redistributed profiles presented in Fig. 6 are expected to be a very good approximation of the true stress profile.

The presence of compressive residual stresses during measurements is not a problem as long as the slot faces do not come into contact, because such situation would violate the linear elastic conditions necessary for the validity of the model. During testing, no contact was observed because the gap between slot faces was wide enough to allow deformation to take place and, therefore, the redistributing residual stress profile presented in Fig. 6 is valid for the conditions of the testing.

However, in practical situations, when a crack is present instead of a slot, the contact forces that arise between the crack faces due to the compressive residual stress field will affect the residual stress profile ahead of the crack tip. In other words, in order to obtain the true redistributing residual stress profile in a cracked component, the zero displacement condition of the crack faces has to be taken into account into the calculations. In fact, the force acting on the crack faces due to compressive stress may even produce a positive stress intensity factor if the crack tip is located into the tensile stress region. Such phenomenon was described in the literature as a "partial crack opening or closure" phenomenon (Ref 24, 25), where a small region near the crack tip (which is immersed in a tensile region) is open, although the calculations based solely on the macroscopic residual stress field indicate a "negative K_r" (or closed crack) for such position. In other terms, the crack tip is in fact experiencing a positive effective K_r value because calculations did not take into account the non-linear contact forces along the crack wake. However, it is important to notice that K_r values will be affected by contact forces only when the crack is fully or partially closed. When the crack is fully open (due to an external applied load or tensile residual stress field, which produce a positive K value), the contact problem does not exist. In this case, K_r is purely described as the result of the macroscopic residual stress profile and the superposition principle remains valid.

These observations are specially important for fatigue crack growth rate predictions in welded plates using methods based on the superposition principle, such as the stress ratio method proposed by Glinka (Ref 26). In this method, the effective K is taken as zero when the sum of the applied $K + K_r$ is negative. In other words, it is assumed that when the crack is closed, there is no contribution to the fatigue crack growth rate. However, such assumption may lead to non-conservative predictions, because contact forces can result in different K_r values as described earlier.

4.2 Longitudinal Slot Testpieces

Figure 7 presents transverse residual stress intensity factors, K_{ry}, obtained for longitudinal slot testpieces. In both cases, i.e., for the slot introduced at 0 and 5 mm from the weld center line, K_{ry} values remain negative in the entire range of acquired data. Additionally, it is possible to observe that K_{ry} profiles varies slightly from one testpiece to another, so that no systematic trend can be established regarding the slot position in relation to the weld center line. However, for both cases, K_{ry} values are much lower than the values obtained in the longitudinal direction, suggesting that cracks growing in a direction parallel to the weld line are likely to be much less affected by the residual stress field produced by the welding procedure.

The initial residual stress profile was also calculated in this case and the results are depicted in Fig. 8. Near the edge of the testpiece, the compressive residual stress can be as high as 120 MPa (~34% of yield strength of parent material). Toward the center of the testpiece, a low magnitude tensile residual stress arises to balance the compressive stresses near the edge. These results indicate that an eventual crack nucleation by fatigue mechanisms is more likely to occur in the center of the

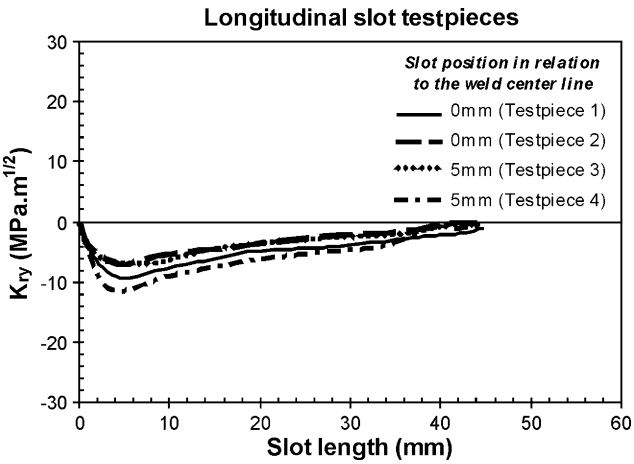

Fig. 7 Residual stress intensity factor profiles for longitudinal slot testpieces

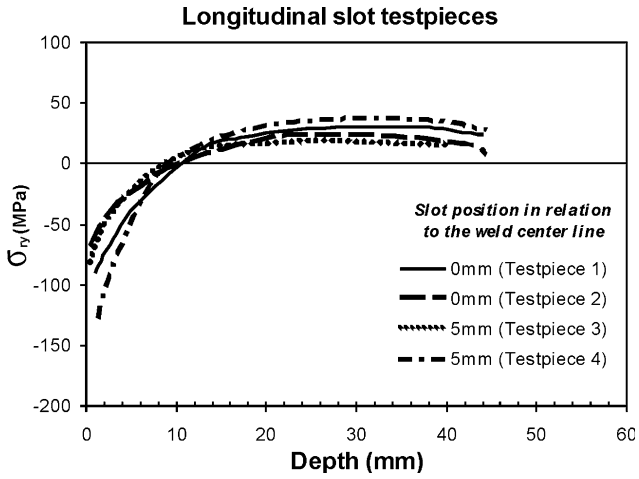

Fig. 8 Residual stress profiles for longitudinal slot testpieces

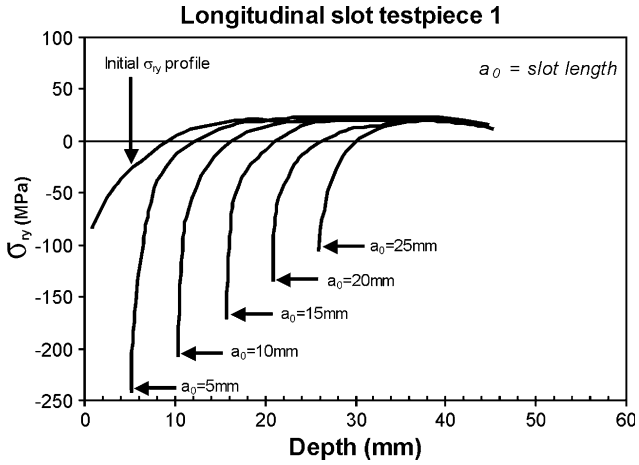

Fig. 9 Residual stress redistribution ahead of the slot tip for longitudinal slot testpiece 1

testpiece. Similar trend was observed by other researchers in friction stir welded aluminum alloys (Ref 22, 23). For testpiece 1, as predicted by the K_{ry} profile, the redistributed residual stress profiles presented in Fig. 9 indicate that a compressive residual stress remains present immediately ahead of the slot tip, reaching a maximum value when the slot is approximately 5 mm long.

These results demonstrate that the inverse weight function method proved to be a valuable tool to understand the stress field behavior in cracked components provided that linear elastic conditions remain valid. If either excessive plasticity or contact between crack faces is present, then appropriate corrections have to be employed in order to provide a more accurate description of the residual stress profile.

5. Concluding Remarks

This work described the determination of the residual stress field in friction stir welded joints of 2024-T3 aluminum alloy plates using the slitting method. It has been concluded that, for the longitudinal direction, the most likely region for fatigue crack nucleation is located on the advancing side of the thermomecanically/heat affected zone, where a peak tensile residual stress value was found. Tensile residual stresses are higher on the advancing side of the weld, probably because of the larger heat input, resulting from the higher relative speed between the tool and the material. On the other hand, transverse residual stresses have a bow-like shape, presenting large compressive residual stresses near the edges of the rectangular testpiece and low magnitude tensile residual stresses in the center of the plate. Residual stress redistribution profiles ahead of the slot tip could be derived using the inverse weight function method. However, for cracked components under compressive residual stress fields, when the crack faces are in contact, the linear elastic conditions necessary for the validity of the method are violated. In this case, the zero displacement condition has to be taken into account in order to provide a more accurate solution of the residual stress field ahead of the crack tip. Further work is required to clarify the trends of residual stress redistribution in cracked components.

Acknowledgments

The authors would like to express their gratitude to Fapesp-Brazil for providing the funds necessary to this research (grants 03/11059-4, 03/10859-7, 03/10858-0, and 02/09027-4). Thanks are also due to EMBRAER (Brazil) for providing the materials used in this work.

References

1. Y.Z. Itoh, S. Suruga, and H. Kashiwaya, Prediction of Fatigue Crack Growth Rate in Welding Residual Stress Fields, *Eng. Fract. Mech.*, 1989, **33**(3), p 397–407
2. G. Bussu and P.E. Irving, The Role of Residual Stress and Heat Affected Zone Properties on Fatigue Crack Propagation in Friction Stir Welded 2024-T351 Aluminium Joints, *Int. J. Fat.*, 2003, **25**(1), p 77–88
3. K.J. Kang, J.H. Song, and Y.Y. Earmme, Fatigue Crack Growth and Closure Through a Tensile Residual Stress Field Under Compressive Loading, *Fat. Fract. Eng. Mat. Struct.*, 1989, **12**(5), p 363–376
4. K.J. Kang, J.H. Song, and Y.Y. Earmme, Fatigue Crack Growth and Closure Behaviour Through a Compressive Residual Stress Field, *Fat. Fract. Eng. Mat. Struct.*, 1990, **13**(1), p 1–13
5. H.C. Choi and J.H. Song, Finite Element Analysis of Closure Behaviour of Fatigue Cracks in Residual Stress Fields, *Fat. Fract. Eng. Mat. Struct.*, 1995, **18**(1), p 105–117
6. M.T. Milan and P. Bowen, Effects of Particle Size, Particle Volume Fraction and Matrix Composition on the Fatigue Crack Growth Resistance of Selectively Reinforced Aluminium Alloys, *Proc. Inst. Mech. Eng. L, J. Mater.: Des. Appl.*, 2002, **216**(4), p 245–255
7. M.T. Milan and P. Bowen, Experimental and Predicted Fatigue Crack Growth Resistance of a Al2124/Al2124+35%SiC Bimaterial, *Int. J. Fat.*, 2003, **25**(7), p 649–659
8. M.T. Milan and P. Bowen, Fracture Toughness of Selectively Reinforced Aluminium Alloys: Pre-Crack Tip in the Composite Side, *Metall. Mater. Trans. A*, 2004, **35A**(4), p 1393–1401
9. M.T. Milan and P. Bowen, Fracture Toughness of Selectively Reinforced Aluminium Alloys: Pre-Crack Tip in the Aluminium Alloy Side, *Mater. Sc. Tech.*, 2004, **20**(6), p 783–789
10. M. Prime, Residual Stress Measurements by Sucessive Extension of a Slot: The Crack Compliance Method, *Appl. Mech. Rev.*, 1999, **52**(2), p 75–96
11. H.J. Schindler, Determination of Residual Stress Distribution from Measured Stress Intensity Factors, *Int. J. Fract.*, 1995, **74**, p R23–R30
12. H.J. Schindler and P. Bertschinger, Some Steps Towards Automation of the Crack Compliance Method to Measure Residual Stress Distributions, *Proceedings of the 5th Inernational. Conference on Residual Stresses ICRS-5*, Vol. 1, T. Ericsson, M. Oden, and A. Andersson, Ed., Linkoping, Sweden, 1997

13. T. Fett and D. Munz, *Stress Intensity Factors and Weight Functions*, Computational Mechanics Publication, Southampton-UK, 1997
14. J.E. Rankin, M.R. Hill, and L.A. Hackel, The Effects of Process Variations on Residual Stress in Laser Peened 7049 T73 Aluminum Alloy, *Mater. Sc. Eng. A*, 2003, **A349**, p 279–291
15. C.N. Reid, A Method of Mapping Residual Stress in a Compact Tension Specimen, *Scr. Metall.*, 1988, **22**(4), p 451–456
16. W. Cheng, I. Finnie, M. Gremaud, and M.B. Prime, Measurement of Near-Surface Residual Stress Using Electric Discharge Wire Machining, *J. Mater. Tech.*, 1994, **116**, p 1–7
17. M.B. Prime and C.H. Hellwig, Residual Stress in a Bi-Material Laser Clad Measured Using Compliance, *Proceedings of the 5th Inernational. Conference on Residual Stresses ICRS-5*, Vol 1, T. Ericsson, M. Oden, and A. Andersson, Ed., Linkoping, Sweden, 1997, p 127-132
18. M.T. Milan, W.W. Filho, A.M.S. Malafaia, B.C. Pelizer, and C.P. Silva, Slot Machining Effects on Residual Stress Measurements Using the Crack Compliance Method, *J. Test. Eval*., 2006, **34**(2), DOI: 10.1520/JTE12700
19. H.J. Schindler, Residual Stress Measurement in Cracked Components: Capabilities and Limitations of the Cut Compliance Method, *Mater. Sc. Forum.*, 2000, **347-349**, p 150–155
20. M. Peel, A. Steuwer, M. Preuss, and P.J. Withers, Microstructure, Mechanical Properties and Residual Stresses as a Function of Welding Speed in Aluminium AA5083 Friction Stir Welds, *Acta Mater.*, 2003, **51**, p 4791–4801
21. C.D. Donne, E. Lima, J. Wegner, A. Pyzalla, T. Buslaps, Investigation on Residual Stresses in Friction Stir Welds, *Proceedings of the 3rd International Symposium on Friction Stir Welding*, TWI, Kobe, Japan, 2001, cd-rom
22. C.D. Donne, G. Raimbeaux, Residual Stress Effects on Fatigue Crack Propagation in Friction Stir Welds, Proc. 10th Int. Conf. Fract., Elsevier Sc. Publ., Hawai, USA, 2001, cd-rom
23. P. Staron, M. Koçak, S. Williams, and A. Wescott, Residual Stress in Friction Stir-Welded Al Sheets, *Physica B*, 2004, **350**, p e491–e493
24. K.J. Kang, J.H. Song, and Y.Y. Earmme, Fatigue Crack Growth and Closure Behaviour Through a Compressive Residual Stress Field, *Fatigue Fract. Eng. Mater. Struct.*, 1990, **13**(1), p 1–13
25. H.C. Choi and J.H. Song, Finite Element Analysis of Closure Behaviour of Fatigue Cracks in Residual Stress Fields, *Fract. Eng. Mater. Struct.*, 1995, **18**(1), p 105–117
26. G. Glinka, Effect of Residual Stress on Fatigue Crack Growth in Steel Weldments Under Constant and Variable Amplitude Load, *ASTM Spec. Tech. Publ.*, 1979, **677**, p 198–214